# Linear Stability of Three-Dimensional Subsonic and Supersonic Swept-Wing Boundary Layers

Sergey A. Gaponov, Viktor Ya. Levchenko, Boris V. Smorodsky

*Abstract:* Stability of three-dimensional swept-wing boundary layers has been investigated in the framework of the linear theory. The most results were obtained for the local self-similar basic flow which was performed within Falkner-Scan-Cooke solution generalized for compressible flows. It has been established that computed subsonic swept-wing boundary-layer stability characteristics correlate well with the experiment. For the supersonic Mach number M=2 boundary layer computations agree with measurements for spanwise scales of the unstable cross-flow disturbances. However theoretical growth rates differ considerably from measured. This difference is explained by high intensity of the initial perturbations excited in the experiment that does not allow to apply linear theory. However the evolution of the natural disturbances of moderate amplitude is predicted well by the theory. It is shown that influence of the compressibility on cross-flow instability modes is insignificant. Also in paper the linear instability of three-dimensional swept-wing boundary layer was studied for a basic flow satisfied to full boundary layer equation. The results difference obtained for self-similar flows and flows satisfied to full boundary layer equation was not more than 15%. Conclusion is made that approximation of local similarity ensures sufficient accuracy and can be applied for simulation of stability experiments at supersonic speeds.

*Key-Words*: compressible boundary layers, laminar-turbulent transition, hydrodynamic stability.

## I. Introduction

Transition to turbulence in a three-dimensional boundary layer on a swept wing has been under investigation during past decades due to its fundamental and practical importance. The review of swept wing boundary layer stability is presented in [1,2]. The latest results in this field are summarized in [3]. Nowadays it is well established, that such boundary layer is subjected to several mechanisms of hydrodynamic instability, each of which is characterized by its own mode and a source of excitation. Cross-flow instability is one of the most important types of the instability responsible for early transition to turbulence on a swept wing. Most results concerning this type of instability were obtained for subsonic velocities. Theoretical research of stability of a compressible three-dimensional boundary layer were started in [4, 5]. Experiments [6] have shown that the distribution of the mean and fluctuating characteristics in the boundary layer at supersonic velocities is approximately the same as that at subsonic speed.

Manuscript received: November 28, 2008.
This work was supported by Russian Foundation for Basic Research (project 08-01-00038-a).
S. A. Gaponov is with the S.A. Khristianovich Institute of Theoretical and Applied Mechanics (ITAM) SB RAS, 630090, Novosibirsk, Russia (phone:+7(383)3301228; fax:+7(383)3307268; e-mail: gaponov@itam.nsc.ru).

A method of passive control of the laminar–turbulent transition on supersonic swept wings was found. It was demonstrated in experiments [7, 8] that the use of artificial microscale roughness periodic in the spanwise direction and located near the leading edge of the wing allows the transition to be shifted downstream. Linear stability theory has been used to predetermine parameters of such passive control process (see [7]).

Experimental investigations of stability of three-dimensional supersonic boundary layers have been performed at Khristianovich Institute of Theoretical and Applied Mechanics [6, 8-10]. To analyze and interpret the experimental data, they have to be compared with the results calculated by the linear theory. Such calculations are also necessary to plan experiments on transition control, as it was done in [7]. This constitutes motivation to perform investigations reported in this paper.

Linear stage of cross-flow instability to steady and traveling low-amplitude perturbations is investigated theoretically. Direct quantitative comparison of theoretical results with experiments conducted earlier at low subsonic speeds [11] and in a supersonic flow [10] is presented.

## II. Linear Stability Analysis

Considering the flow in the boundary layer on an infinite-span swept wing model and its stability, one can reasonably use two commonly accepted coordinate systems (Fig.1). The system $(s, z^*)$ is fitted to the model (the origin is on the leading edge of the wing). The $s$ coordinate is directed along the chord over the model contour, and the $z^*$ coordinate is directed over the wing span parallel to its leading edge. This coordinate system is used to calculate the

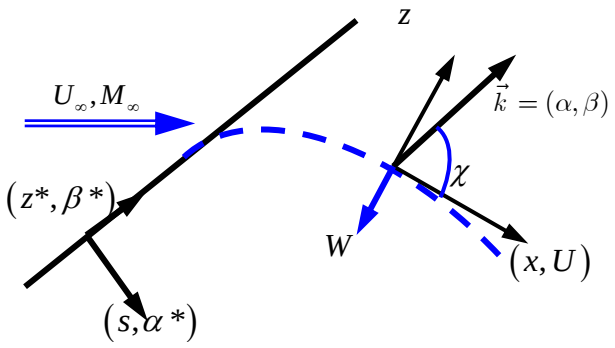


**Fig.1**: Geometry of the swept wing and coordinate systems used: the dashed curve is the streamline; the secondary flow velocity is indicated by $W$ .

mean flow characteristics, because its parameters are independent of $z^*$. It is more convenient, however, to calculate the stability characteristics in a local coordinate system $(x,z)$, where the $x$ coordinate is directed along the local velocity vector of the potential flow on the boundary-layer edge. In all coordinate systems mentioned, the $y$ axis is aligned normal to the model surface.

Within the framework of the linear stability theory, we can present the flow field in a compressible boundary layer as a sum of the mean flow and a weak perturbation:

$$\mathbf{u} = U_\infty \left( \mathbf{U}(x,y) + \varepsilon \mathbf{V}(x,y,z,t) \right) , \qquad (1)$$

Here the mean flow velocity $\mathbf{U}(x,y) = \left(U(x,y),0,0\right)$ is considered in the approximation of local parallelism, $\varepsilon \mathbf{V} = \varepsilon(u,v,w)$ are the components of the velocity disturbance, and $\varepsilon << 1$ is a small parameter characterizing the disturbance amplitude. The expressions for the temperature $T$, pressure $P$, and density $\rho$ are written in a manner similar to (1). The equations for disturbances are obtained by substituting (1) into the Navier–Stokes, continuity and energy equations. In the present work, we consider a three-dimensional problem of stability, where the frequency is assumed to be a real quantity, while the streamwise wavenumber is assumed to be a complex quantity. An analysis of stability of the boundary-layer flow on a swept wing in the local parallel approximation usually involves the assumption that the amplitude of localized disturbances increases in the external flow direction $x$, and disturbances periodic in terms of $z^*$ increase along the chord s [12]. The location of the neutral stability curves is independent of the direction of growth of disturbances. Following [12], we assume that the direction of growth of all disturbances coincides with the direction of the external flow streamline. The solution of the problem is presented as

$$\vec{\mathrm{q}} = A(x)\vec{\phi}(y) \exp\left( i\int_{x_0}^{x} \alpha(x')\,dx' + i\beta z - i\omega t \right) ,$$

where $\vec{k} = (\alpha, \beta)$ is the wave vector consisting of the streamwise $\alpha$ and spanwise $\beta$ wavenumbers; $\omega = 2\pi f$; $f$ is the frequency; the sought vector $\vec{\phi}$ is presented as

$$\vec{\phi} = (u,v,w,p,\theta)^T , \qquad (2)$$

i.e., it consists of three components of the velocity disturbance, pressure disturbance, and temperature disturbance, whereas the disturbances of density and mass flow $A$ are expressed via the components of the vector $\vec{\phi}$. In (2), all quantities are normalized to appropriate parameters of the mean flow outside the boundary layer. In the first approximation in terms of $\varepsilon$, we obtain the linear boundary-value problem

$$\frac{d\vec{\phi}}{dy} = H\vec{\phi} , \qquad (3)$$

$$(u,v,w,\theta) = 0 , \ (y=0), \ \left|\vec{\phi}\right| < \infty , \ (y \to \infty), \qquad (4)$$

where $H$ is the linear operator generalizing the Lees–Lin operator to the case of a three-dimensional boundary layer. The nonzero elements of $H$, taken from [1], are presented in the Appendix. These elements depend both on the mean flow properties (velocity and temperature profiles, Mach number $\mathrm{M}$, Reynolds number $\mathrm{Re}$, and Prandtl number $\mathrm{Pr}$) and on the wave parameters (frequency and wavenumbers). The homogeneous boundary conditions (4) are satisfied only under certain combinations of these parameters, which have to be found. Thus, (3-4) form an eigenvalue problem.

Stability of the flows under considerations was analyzed in the present work by means of numerical integration of system (3-4) by the method of orthonormalizations [13]. Streamwise wavenumber $\alpha = \alpha_\mathrm{r} + i\alpha_\mathrm{i}$ was found as the eigenvalue of the boundary-value problem, and the components of the vector $\vec{\phi}$ are the corresponding eigenfunctions. The conditions $-\alpha_\mathrm{i} > 0$ and $-\alpha_\mathrm{i} \le 0$ refer to unstable disturbances amplifying in the downstream direction and to stable waves decaying with increasing $x$.

In the case of weak streamwise mean flow nonparallelism (inhomogeneity) the parameters $A$ and $\varphi$ are also slow functions of streamwise coordinate $x$. In these cases parabolized stability equations (PSE) should be applied [14].

Mean flow in most simple cases could be obtained analytically, as in [15**]**. In more complicated flows one can use direct numerical simulations (DNS) [16].

The mean flow in a three-dimensional boundary layer on an infinite-span swept wing can be theoretically described in the approximation of the so-called local self-similarity [17]. Within such a model, the boundary-layer equations are reduced to a system of ordinary differential equations by introducing the Dorodnitsyn–Lees variables, depending on the local Mach number $\mathrm{M}_e$ and on the streamwise pressure gradient of the inviscid external flow outside the boundary layer:

$$\xi = \int_0^s \rho_\mathrm{e}\mu_\mathrm{e}U_\mathrm{e}\,ds , \ \eta = \frac{\rho_\mathrm{e}U_\mathrm{e}}{\sqrt{2\xi}} \int_0^y \frac{\rho}{\rho_\mathrm{e}}\,dy ,$$

where $U_e$ is the streamwise (along $s$) velocity component outside the boundary layer and $\mu_e$ is the viscosity). Assuming that the mean flow parameters are independent of $z^*$, we can present the stream function, the streamwise and spanwise components of velocity, and enthalpy in the form

$$\psi(s,\eta) = \Phi(s) f(\eta) , \ U(s,\eta) = U_\mathrm{e}(s) f'(\eta) ,$$
$$W(s,\eta) = W_\mathrm{e}(s) q(\eta) , \ I(s,\eta) = I_\mathrm{e}(s) g(\eta) ,$$

where the prime means the derivative with respect to the coordinate $\eta$, normal to the model surface. Thus, in the approximation of local self-similarity, we obtain a system that describes the flow in a three-dimensional boundary layer:

$$(Cf'')' + ff'' + \left[ \frac{\rho_\mathrm{e}}{\rho} - (f')^2 \right] \beta_\mathrm{H} = 0 , (Cq')' + fq' = 0 ,$$

$$\left( \frac{C}{\mathrm{Pr}} g' \right)' + fg' = \frac{1-\mathrm{Pr}}{\mathrm{Pr}} \frac{(\gamma-1)\mathrm{M}^2}{1 + \dfrac{(\gamma-1)}{2}\mathrm{M}^2} \times , \qquad (5)$$

$$\times \left[ C\left( f' f'' \cos^2 \lambda_e + qq' \sin^2 \lambda_e \right) \right] ,$$

Here $\lambda_e$ is the local sweep angle, i.e., the angle between the axis $s$ and the local direction of the external flow velocity $U_p$, $\gamma$ is the ratio of specific heats, $C = \frac{\rho\mu}{\rho_e\mu_e}$, and $\beta_H = \frac{2\xi}{U_e}\frac{dU_e}{d\xi}$. System (5) is derived under the assumption that the parameters $\beta_H$ and $M_e$ are independent of the streamwise coordinate $\xi$. If these parameters depend only weakly on $\xi$, the system (5) has to be applied locally, and its solutions $(f, q, g)$ will parametrically depend on the streamwise coordinate.

In the absence of the boundary-layer suction on the surface, the boundary conditions for a thermally insulated model can be written as

$$(f, f', q, g') = 0, (\eta = 0), (f', q, g) \to 1, (\eta \to \infty) \quad (6)$$

System (5) is the generalization of the Falkner–Scan–Cooke equations to the flow in a compressible

boundary layer. In the present work, system (5-6) was numerically integrated by the fourth-order Runge–Kutta method. The shooting method was used to satisfy the boundary conditions.

## III. Stability of Self-Similar Boundary Layer

The mean flow and stability were calculated for $\Pr = 0.72$ and $\gamma = 1.4$. Some results calculated for steady $(f = 0)$ modes of instability of the transverse flow in subsonic and supersonic three-dimensional boundary layers are presented below.

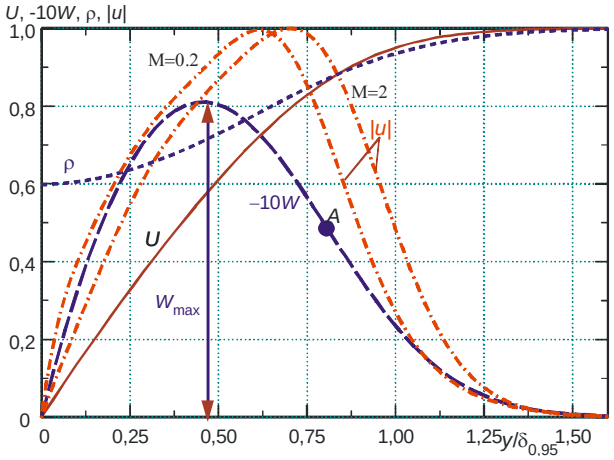


**Fig.2**: Mean flow parameters for $M_e = 2$ and fluctuations of the longitudinal velocity of the steady $(\omega = 0)$ model of instability of the transverse flow for $\beta = 1.3$ and $R = 5000$.

Fig.2 shows the calculated distributions normal to the model surface for the mean strewmwise velocity $U = U(y)$, velocity of the secondary or cross-flow $W(y)$, and density $\rho = 1/T$ for $M_e = 2$ (the local values of $U, W$ and $\rho$ are normalized to the corresponding values outside the boundary layer). The normal coordinate is brought to dimensionless form on the basis of the boundary-layer thickness $\delta_{0.95}$: $U(y = \delta_{0.95}) = 95\% U_e$. For chosen parame–ters, the changes in the mean density inside the boundary layer stays within 40%. The favorable pressure gradient $(\beta_H > 0)$ typical for the initial part of the swept wing (closer to the leading edge) is responsible for the formation of a cross-flow with $W(y) < 0$. The profile $W(y)$ acquires an inflection (point *A* in Fig.2), which leads to substantial destabilization of the flow. An important parameters characterizing instability of the three-dimensional boundary layer considered is the amplitude of the secondary flow $W_{max}$ determined as magnitude of the cross-flow in its maximum: $W_{max} = \max_{0 \le y < \infty} |W(y)|$. In the present case, the secondary flow with $W_{max} \approx 0.08$ 1 was obtained for $\lambda = 45^\circ$ and $\beta_H \approx 0.29$.

The dot-dashed curves in Fig.2 show the profiles of fluctuations of the streamwise disturbance velocity $|u(y)|$ (normalized to the maximum values) at $M_e = 2,0$ and $0,2$. The difference in these functions for subsonic and supersonic flow regimes is insignificant and is manifested only in a small shift of the location of the maximum of fluctuations, which correlates well with the shift of the inflection point on $W(y)$.We calculated stability diagrams for steady and unsteady cross-flow instability modes for variety of situations: for different Mach numbers, different values of the secondary flow amplitudes.

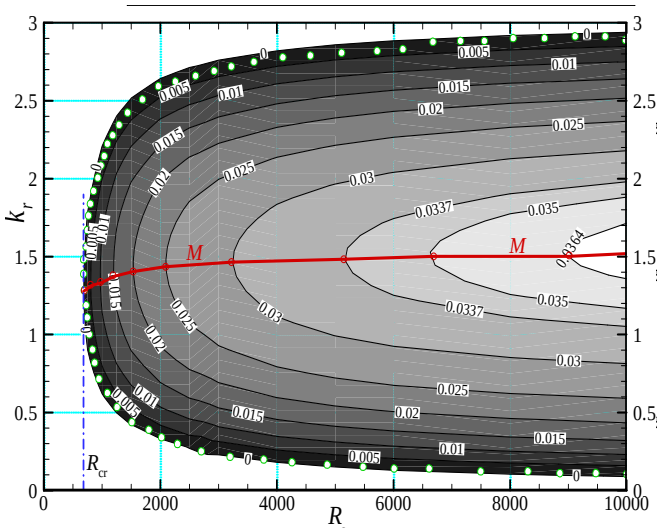


**Fig.3**: Stability diagram of stationary modes at $M_e = 2.0$, $W_{max} = -0.08$: growth rate contours $-\alpha_i \delta_{0.95}$.

Fig.3 presents the stability diagram for stationary $(\omega = 0)$ cross-flow instability modes at $M_e = 2.0$, $W_{max} = -0.08$, i.e. contours of spatial growth rates on the plane $(R, k_r)$, where $R = \rho_e U_e \delta_{0.95} / \mu_e$ is the Reynolds number based on the boundary layer thickness $\delta_{0.95}$ and $k_r = \sqrt{\alpha_r^2 + \beta^2}$ is the magnitude of the wave vector. The instability region $(-\alpha_i > 0)$ is shaded. Position of the neutral stability curve $(\alpha_i = 0)$ is in a good agreement with computations [12], shown at Fig.3 by small circles. Critical Reynolds number

for this case is $R_{cr} \approx 680$. Computations show, that with increasing $W_{\max}$ critical Reynolds number decreases. At $W_{\max} \geq 0.04$ the range of unstable wave numbers in the adopted normalizations is concentrated in the range $0 < k_r < 3$ and is almost independent of $R$ and M. This is a typical indication of the inviscid cross-flow instability modes developing on the inflectional mean velocity profile. In the absence of the cross-flow (in a two-dimensional boundary layer) stationary modes cannot amplify.

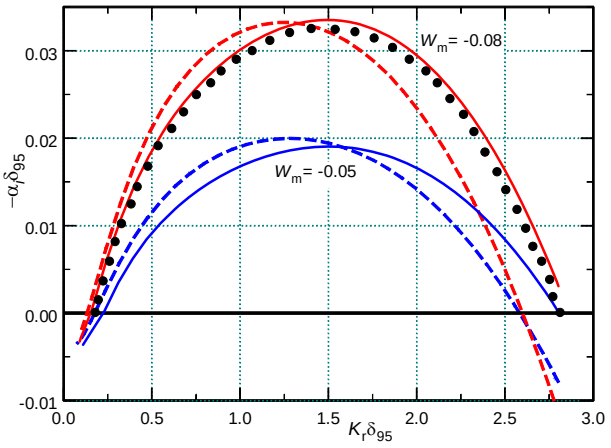


**Fig.4**: Spatial growth rates of stationary modes for $W_{\max} = -0.08$ and $-0.05$ at $M_e = 2.0$ (solid lines) and $M_e = 0.2$ (dashed lines), $R = 5000$.

Calculations of the stability diagram for stationary modes at different Mach numbers have shown that the instability region and growth rates depend only weakly on Mach number M. Fig.4 demonstrates comparison of spatial growth rates of steady modes at $W_{\max} = -0.08$ and $-0.05$ for Mach numbers $M_e = 2.0$ (solid lines) and $M_e = 0.2$ (dashed line), $R = 5000$. Computations [12] are shown at this diagram by circles and agree well with our data. Growth of $|W_{\max}|$ leads to the amplification of instability, while compressibility influence is very weak and is visible only in a small shift of curves maxima positions while their magnitude for $M_e = 2.0$ and 0.2 differs less than on 10%. Wave vector of amplifying disturbances has an orientation almost normal to the direction of outer flow.

## IV. Validation of Theory Verusus Measurements Performed in the Subsonic Flow

Gaponenko et al. [11] experimentally studied the linear stage of evolution of transverse flow instability at a subsonic flow velocity. In the initial cross sections of the swept wing, the mean flow was modeled with the use of a flat plate with an induced favorable pressure gradient. The flat plate was mounted in the wind-tunnel test section at a sweep angle $\lambda = 25^\circ$. The pressure gradient was generated by a dummy wall placed into the test section. The experiments were performed in a T-324 low-turbulence wind tunnel based at the Khristianovich Institute of Theoretical and Applied Mechanics. The flow field in the boundary layer was recorded by a hot-wore anemometer. The cross-flow instability modes were artificially excited in the boundary layer by various generators of disturbances operating at frequencies $f = 8,3; 25,0; 35,0$ Hz. The characteristics of stability of normal modes were obtained by a frequency-wave spectral analysis.

The conditions of the present linear stability calculations were the same as those used in the experiments [11]. The following parameters obtained in the experiments were used: velocity at the boundary-layer outer edge $U_e \approx 6,8$ m/sec, displacement thickness $\delta_1 \approx 1,25$ mm, Hartree parameter $\delta_H \approx 0,47$, and calculated Reynolds number $\mathrm{Re}_{\delta_1} \approx 560$.

Theoretical results for conditions of these experiments are presented at Figs.5,6. Fig.5 shows the example of the dispersion relation of normal cross-flow instability modes, in the form of wave propagation angle $\chi = \mathrm{arctg}(\beta/\alpha_r)$ versus spanwise wave number $\beta$ for frequency $f = 35$ Hz. For large values of $|\beta\delta_1| > 0.4$ wave angles are close to $\pm 90^\circ$. At smaller $\beta$ there is a range of continuous change of $\chi$ between these two limiting values. With reduction of $f$ the range of $\beta$ of such passage decreases and at zero frequency (stationary disturbances) there is only a jump from $\chi \approx -93^\circ$ to $\chi \approx 87^\circ$. These values differ on $180^\circ$ and correspond to the same angle of stationary cross-flow vortices for all $\beta$. It is worth to mention a good quantitative agreement of theory and experiment, presented at Fig.5.

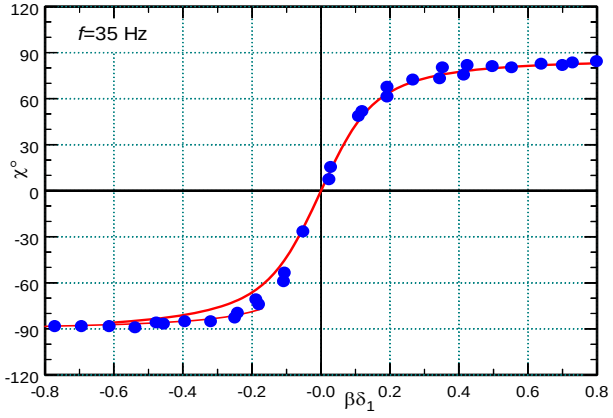


**Fig.5**: Wave vector orientation of cross-flow instability modes versus spanwise wave number, $f = 35$ Hz. Comparison of the theory (curves) and experiment (symbols).

Fig.6 demonstrates comparison of the computed and measured spatial growth rates of normal cross-flow instability modes for $f = 35$ Hz. Positive values of $\beta$ correspond to waves propagating almost against the direction of secondary flow (because $W(y) < 0$), whereas disturbances with $\beta < 0$ propagate *in* the direction of the secondary flow. Calculations show that for $f = 35$ Hz the BL is stable for all $\beta$. Despite the rather wide scattering of experimental points at Fig.6 the theoretical curve is in a satisfactory agreement with measured values.

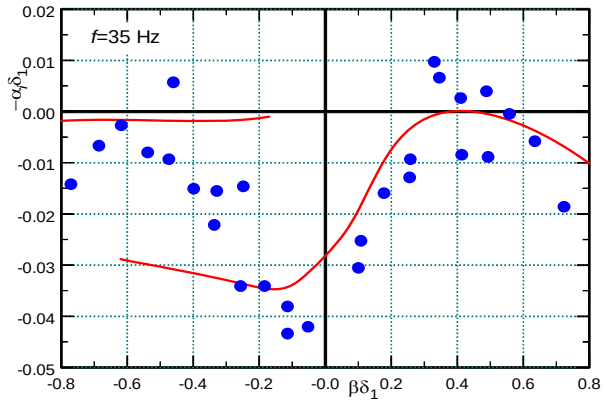


**Fig.6**: Spatial growth rates versus spanwise wave number, $f = 35$ Hz. Comparison of the theory (curves) and experiment (symbols).

Quasi-2D waves (with $\beta$ close to zero) are strongly decaying. The most unstable modes are concentrated in narrow band of wave angles close to $\pm 90^\circ$ $(\beta\delta_1 \approx 0.4)$. The characteristic width of these regions decreases with frequency reduction. In the region of negative values of a spanwise wave number there is a range of $-0.6 < \beta\delta_1 < -0.2$ where theoretical determination of growth rates gives ambiguous results. Presence of two modes of a discrete spectrum was revealed, one of which has much higher attenuation rate than the other. One possible explanation to this phenomenon is that the mode with greater decrements at $\beta < 0$ is closer to the Tollmien-Schlichting instability mode, distorted by the presence of the secondary flow. This assumption is confirmed also by the calculated value of its phase velocity $c = \omega/\alpha_r \approx 0.3$ (for $\beta = 0$) typical for this instability waves. However in the flow considered, Tollmien-Schlichting instability is suppressed by a strong streamwise pressure gradient $(\beta_H > 0)$ and in the result these waves decay fast in the downstream development. In this range of $\beta$ the experimental values are located between two theoretical curves. It gives grounds to assume, that disturbance generators used in measurements, have excited simultaneously disturbances of both kinds, and the hot-wire anemometer has registered their mixture.

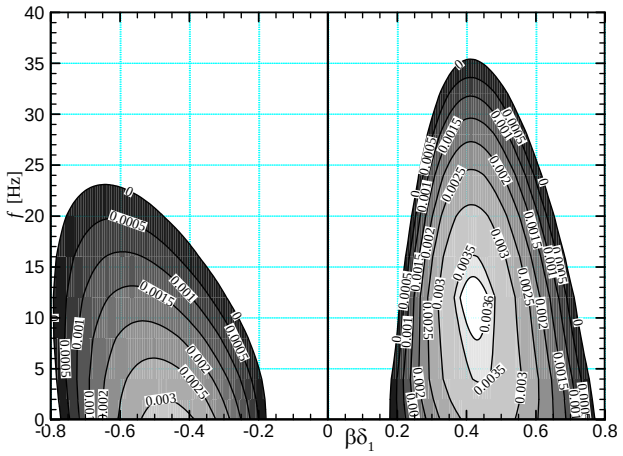


**Fig.7**: Spatial growth rate contours in the local system on the plane $(f, \beta)$.

Next Fig.7 shows the cumulative theoretical stability diagram of the flow under investigation, i.e. spatial amplification rates on the plane frequency – spanwise wavenumber. The region of instability at $\beta > 0$ is considerably larger. Disturbances with $f \approx 12$ Hz and $\beta\delta_1 \approx 0.43$ have maximal growth, while waves propagating in the direction of the cross-flow $(\beta < 0)$ have much smaller growth rates.

## V. Comparison of Computations with Experiments Performed in the Supersonic Flow

The main goal of the present work was to model the experiments which have been performed earlier at ITAM SB RAS [9,10]. Measurements have been performed in the low-noise supersonic wind tunnel T-325 based at the Khristianovich Institute of Theoretical and Applied Mechanics of the Siberian Division of the Russian Academy of Sciences at a free-stream Mach number $M_\infty = 2$ and Reynolds number per meter $Re_1 = 6,6 \cdot 10^6$ m$^{-1}$. A wing model with a symmetric lenticular profile and a sweep angle $\lambda = 40^\circ$ was used. Controlled disturbances have been excited in the boundary layer on the model from a localized source on the basis of a glow discharge generator. The discharge ignition frequency was 10, 20, and 30 kHz. The mass-flow fluctuations were recorded by a constant-temperature anemometer. Frequency-wave and amplitude-phase spectra of disturbances in several cross sections along the streamwise coordinate $s$ were obtained by applying a discrete Fourier transform. The evolution of disturbances at the excited frequencies was found to be similar to the evolution of traveling waves at subsonic flow velocities. The results calculated by the linear stability theory are compared with experimental data.

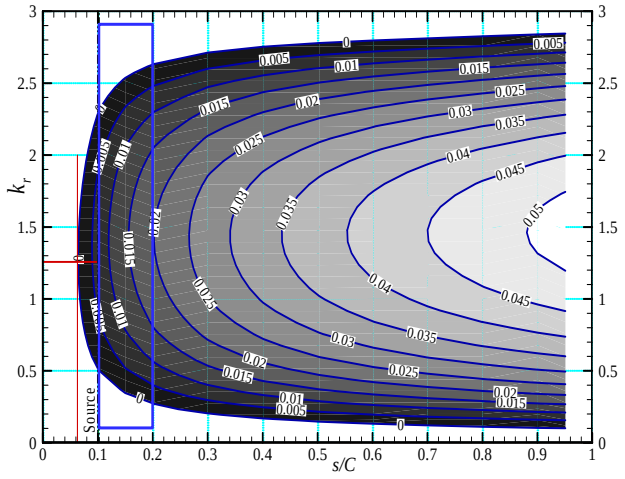


**Fig.8**: Contours of cross-flow disturbance spatial growth rates $-\alpha_i\delta_{0.95}$ in supersonic swept wing BL for stationary disturbances in the plane $(s/C, k_r)$.

In the present work, the characteristics of the outer flow over the wing have been computed according to Prandtl-Mayer expansion flow formulas. Calculations show continuous isentropic expansion of the flow along the whole wing chord, so calculated local Mach number is increasing from $M_e \approx 1.6$ at $s = 0$ up to 2.36 on a trailing edge of the

wing $(s/C=1)$, where $C$ is the model chord. The local sweep angle monotonically decreases from $\lambda \approx 47^\circ$ to $\lambda \approx 36^\circ$. Hartree parameter grows from $\beta_H = 0$ to $\beta_H = 0.74$. The boundary layer on the model surface has been computed using distributions $\lambda(s), \beta_H(s), M_e(s)$ in the approximation of local self-similarity [17,18]. It has been found, that the values of $W_{max}$ increase from zero to $W_{max} \approx -0.12$ in the downstream direction.

The linear stability of the three-dimensional boundary layer on the swept wing model under investigation showed that the instability region begins close to the leading edge of the model $(s/c \approx 0,06)$. The growth rates of steady modes continuously increase in the downstream direction until the trailing edge.

Fig.8 shows contours of disturbance spatial growth rates along the wing chord $s/C$ and $k_r$ in relation to stationary disturbances. The unstable region is shaded, its beginning is located close to the model leading edge. Amplification rates continuously grow downstream up to the trailing edge. The disturbance generator has been located in the beginning of unstable region and its location is marked by the vertical line. The field of stability measurements is marked at the diagram by a rectangle. Conditions of these experiments were so, that computed spatial linear amplification rates were much higher in comparison with subsonic experiment (Fig.7).

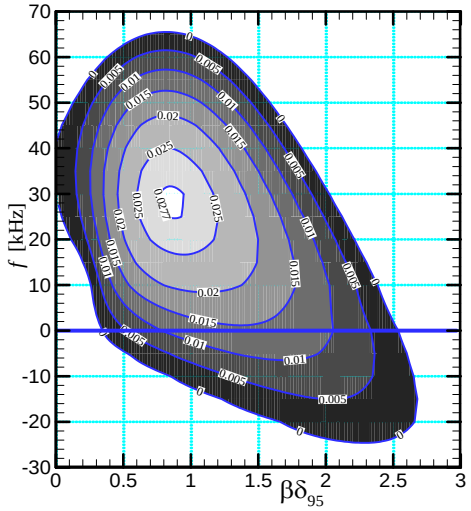


**Fig.9**: Contours of cross-flow disturbance spatial growth rates $-\alpha_i \delta_{0.95}$ in supersonic swept wing BL in the plane $(f, \beta)$ at $x/C \approx 0.15$.

Fig.9 shows also theoretical stability diagram – spatial growth rate contours on the plane $(\beta, f)$ at $x/C \approx 0.15$ ($s = 30$ mm). Negative frequencies at this diagram correspond to the waves propagating in the direction of secondary flow, i.e. correspond to $\beta < 0$. It is seen, that the maximal growth at this section $s$ is for traveling waves with frequency $f \approx 29$ kHz and $\beta\delta_{0.95} \approx 0.8$, and their amplification rates are almost double of maximum rates for stationary modes $(f = 0)$. The range of unstable frequencies propagating in the direction opposite to the secondary (cross-) flow $(\beta > 0)$ is approximately $0 \le f < 65$ kHz, which is in qualitative agreement with the experimental results [10], where amplification of natural background disturbances with frequencies $0 \le f < 65$ kHz was observed. Instability region corresponding to $\beta < 0$ is noticeably smaller.

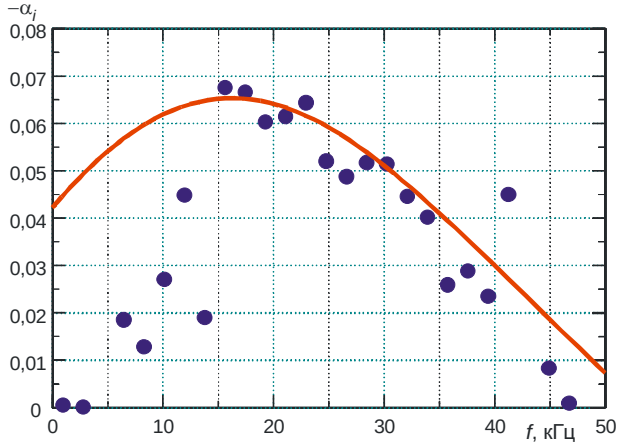


**Fig.10**: Spatial growth rates of the spectral components of natural disturbances: the curve and the points are the calculated results and the experimental data [10].

The calculated and measured spatial growth rates are plotted in **Fig.10**. The experimental points were obtained by means of differentiation of the measured spectra of natural disturbances of the boundary layer on the swept wing model over the longitudinal coordinate (see Fig.2a in [10]), while the theoretical curve was constructed over the maximum values $-\alpha_{i,\max} = \max_{\beta}\left[-\alpha_i(f,\beta)\right]$ determined from the stability diagram. The theoretical and experimental data are seen to agree well at high frequencies $15 \le f \le 50$ kHz. At low frequencies ($f < 15$ kHz), the measured growth rates are substantially smaller. A possible reason is the dominating contribution of external acoustic disturbances (wind-tunnel noise) into the low-frequency part of the spectrum; the intensity of these acoustic disturbances depends weakly on the streamwise coordinate, and their growth rates are small.

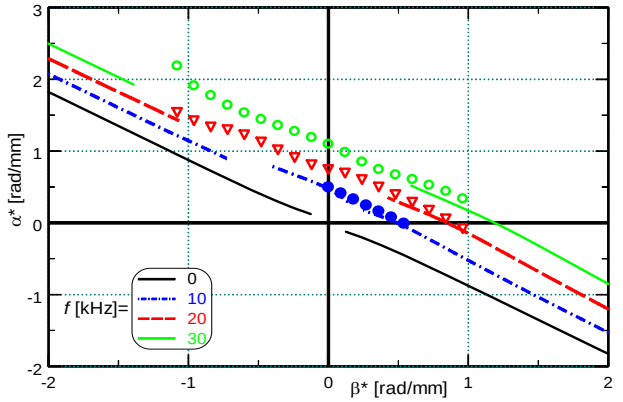


**Fig.11:** Streamwise wave number of normal instability modes as a function of spanwise wave number (dispersion relation). Comparison of the theory (curves) with measurements (symbols).

Comparison of theory with measurements performed with artificially excited disturbances is presented at Figs.11,12.

Fig.11 shows dispersion relation curves $\alpha^* = \alpha^*(\beta^*)$ computed in the coordinate system $(s, z^*)$ for frequencies $f = 0, 10, 20, 30$ kHz. In the examined range of parameters, theoretical results are in good quantitative agreement with experiment in the studied field of parameters.

Fig.12 presents spatial growth rates versus spanwise wave number at $s = 30$ mm. Experimental data [10] are shown by symbols for frequency $f = 10$ kHz at this plot. In contrast to dispersion relations (Fig.7) theoretical results deviate much from experiment. The range of the most amplifying disturbances in experiment is $0.3 < \beta^* < 1.2$ rad/mm, whereas according to the linear theory maximum growth should be for disturbances with $2 < \beta^* < 3$ rad/mm.

Reasons of such discrepancy can be explained by the initial conditions realized in experiment. The amplitude of mass flux perturbation excited in the experiment, reached 30% of the mean value. Also strong distortion of the mean flow was detected [3], that is an indication of strong nonlinearity of a disturbance field. Therefore the use of the linear theory is limited. In addition, the range of the initial (in terms of the coordinate $z^*$) disturbance was rather large in the experiments, i.e., waves with low values of $\beta^*$ dominated in the wave spectrum of the initial disturbances at the generation frequency. It was the growth of these disturbances that was registered in the downstream direction.

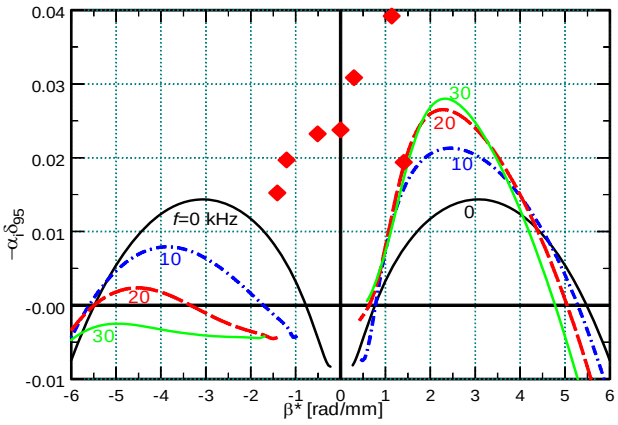


**Fig.12**: Spatial growth rates versus $\beta^*$ [rad/mm], ($s = 30$ mm). Symbols – experimental data [10] at $f = 10$ kHz.

There seem to be some other reasons for the dominating growth of modes with $\beta^* \approx 0$. The experiments [20] performed in a two-dimensional boundary layer on a flat plate at $M = 2$ and larger intensities of initial disturbances also revealed the predominant growth of two-dimensional fluctuations, whereas it is three-dimensional linear disturbances that increase most rapidly in a supersonic boundary layer. This fact was explained in [21], where the evolution of disturbances of higher intensities in a supersonic boundary layer is demonstrated to be determined by the presence of steady disturbances responsible for distortions of the mean fields. As a result, two-dimensional components of the disturbance spectrum are mainly amplified. Apparently, the higher initial amplitude of transverse flow instability modes excited in a three-dimensional boundary layer on a swept wing in the experiments [10] also excites deformations of the mean flow, and the measured characteristics of stability of such a flow differ from those calculated by the linear theory.

Thus, the calculated transverse scales of disturbances of the secondary flow are demonstrated to agree well with experimental data on stability of a three-dimensional supersonic boundary layer with artificial disturbances at M = 2. The calculated growth rates of disturbances, however, differ from the measured values. At the same time, the linear stability theory offers an adequate description of the development of natural disturbances whose amplitudes are much lower than the amplitudes of artificial disturbances.

To verify the applicability of the local-similarity approximation for mean flow computations in three-dimensional infinite swept wing boundary layer we have performed also a numerical simulation of the boundary layer flow on the basis of non-similar boundary-layer equations. Full partial-derivative compressible laminar boundary layer equations for infinite swept-wing have been integrated numerically by means of finite-difference Keller box scheme [22]. Comparison of boundary-layer mean velocity and temperature profiles computed for conditions of swept-wing experiments [10] in the framework of local similarity approximation as well as in non-similar boundary layer solution have shown that boundary layer thickness $\delta = \delta(x)$ for nonsimilar equations is slightly thicker in comparison to the local similarity solution, while the amplitude of the cross-flow $|W_{\max}| = |W_{\max}(x)|$ becomes slightly smaller. These two factors affect stability characteristics of the boundary layer flow. Indeed, a thickening of the boundary layer means growth of the Reynolds number, that leads to destabilization, while reduction of $|W_{\max}|$ leads to a certain flow stabilization. As a result, stability characteristics of the flow, computed by these two approximations, are close to each other.

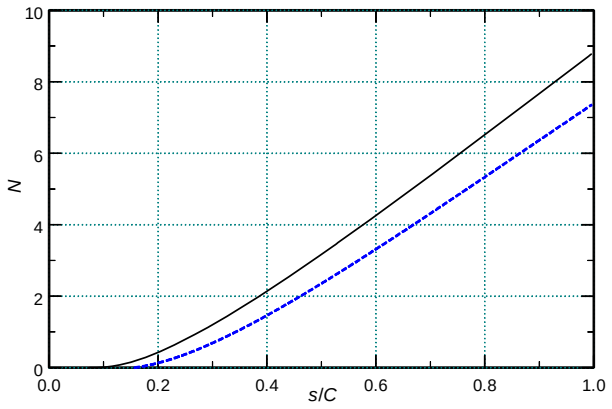


**Fig.13**: Growth curves (N-factors) of stationary $(\omega = 0)$ cross-flow instability modes, computed for conditions of measurements [10]: local self-similar solution (solid line) and full boundary layer solution (dashed line); spanwise wave length $\lambda = 2\pi/\beta = 7$ mm.

This fact is demonstrated at Fig.13, where amplification

curve (*N*-factor) $\left(N=-\int_{s_0}^{s}\alpha_i(s')ds'\right)$ is plotted versus streamwise coordinate for stationary cross-flow instability mode computed in the approximation of the local similarity (solid line). The growth curve obtained from nonsimilar boundary-layer equations (dashed line) shows slightly smaller growth in comparison to the mean flow computed in the local similarity approximation. However this difference is not large and close to the trailing edge of the model $(x/C\approx 1)$ it is less than 15%.

Distribution of the N-factors versus spanwise wavenumber is shown at Fig.14 for the middle section of the wing chord $(s/C=0.5)$. One can see that the N-factors computed by the two approximations at this streamwise section have maxima located around $\beta\approx 2$ rad/mm, but they do not coincide. However maximal $N_{\max}\approx 4.3$ are about the same for both approximations. Therefore one can make a conclusion that the approximation of local self-similarity accepted in the most part of the present paper is accurate enough and can be used to simulate theoretically stability experiments performed on a swept wing in a supersonic flow.

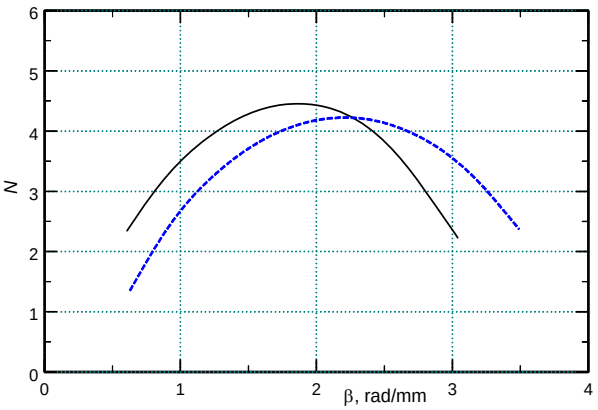


**Fig.14**: N-factors of stationary $(\omega=0)$ cross-flow instability modes versus spanwise wavenumber, $(s/C=0.5)$: local self-similar solution (solid line) and full boundary layer solution (dashed line).

## VI. CONCLUSION

Stability of compressible three-dimensional swept-wing boundary-layer was studied in the framework of the linear stability theory. The analysis was based on the approximation of local self-similarity of the mean flow and was conducted with Falkner-Scan-Cook solution extended to compressible flows. It was shown that compressibility influence on the cross-flow instability modes is insignificant. Good quantitative agreement of all computed stability characteristics with experimental data obtained in T-324 for the subsonic BL is received. For supersonic-swept wing BL at Mach number $M=2$ a good agreement of the theory with measurements performed in T-325 has been obtained only for spanwise scales of cross-flow vortices. However computed growth rates differ significantly from measurements. This discrepancy is explained by too high initial amplitude of disturbances excited in experiment, that is outside of a linear stability theory applicability range. Conclusion is made that approximation of local similarity ensures sufficient accuracy and can be applied for simulation of stability experiments at supersonic speeds.

## APPENDIX

Nonzero elements of the matrix $H$ in (3) are :

$$H_{12}=H_{56}=H_{78}=1\ ,$$

$$H_{21}=\alpha^2+\beta^2+i\frac{\xi R}{\mu T}\ ,\quad H_{22}=-\frac{D\mu}{\mu}\ ,$$

$$H_{23}=\frac{R\,DU}{\mu T}-i\alpha\left[l_1\frac{DT}{T}+\frac{D\mu}{\mu}\right],$$

$$H_{24}=i\frac{\alpha R}{\mu}-\alpha l_1\gamma M^2\xi\ ,$$

$$H_{25}=l\xi\frac{\alpha}{T}-\frac{D(\mu' DU)}{\mu}\ ,$$

$$H_{26}=-DU\frac{\mu'}{\mu}\ ,\quad H_{31}=-i\alpha\ ,\quad H_{33}=\frac{DT}{T}\ ,$$

$$H_{34}=-i\gamma M^2\xi\ ,\quad H_{35}=i\frac{\xi}{T}\ ,\quad H_{37}=-i\beta\ ,$$

$$H_{41}=-i\alpha\chi\left[l_2\frac{DT}{T}+2\frac{D\mu}{\mu}\right],\quad H_{42}=-i\alpha\chi\ ,$$

$$H_{43}=\chi\left[l_2\left(\frac{D\mu\,DT}{\mu T}+\frac{D^2T}{T}\right)-\left(i\frac{\xi R}{\mu T}+\alpha^2+\beta^2\right)\right],$$

$$H_{44}=i\chi\gamma M^2 l_2\left[\xi\left(\frac{D\mu}{\mu}+\frac{DT}{T}\right)+\alpha DU+\beta DW\right],$$

$$H_{45}=i\chi\left[(\alpha DU+\beta DW)\left(\frac{l_2}{T}+\frac{\mu'}{\mu}\right)+\xi l_2\frac{D\mu}{\mu T}\right],$$

$$H_{46}=i\chi l_2\frac{\xi}{T}\ ,\quad H_{47}=-i\beta\chi\left[l_2\frac{DT}{T}+2\frac{D\mu}{\mu}\right],$$

$$H_{48}=-i\beta\chi\ ,\quad H_{62}=-2\,\mathrm{Pr}(\gamma-1)M^2DU\ ,$$

$$H_{63}=R\,\mathrm{Pr}\frac{DT}{\mu T}-2i(\gamma-1)M^2\,\mathrm{Pr}(\alpha DU+\beta DW)\ ,$$

$$H_{64}=-iR\,\mathrm{Pr}(\gamma-1)M^2\frac{\xi}{\mu}\ ,\quad H_{64}=-iR\,\mathrm{Pr}(\gamma-1)M^2\frac{\xi}{\mu}\ ,$$

$$H_{65}=iR\,\mathrm{Pr}\frac{\xi}{\mu T}+\alpha^2+\beta^2-(\gamma-1)M^2\,\mathrm{Pr}\frac{\mu'}{\mu}$$

$$\left(DU^2+DW^2\right)-\frac{D^2\mu}{\mu}\ ,\quad H_{66}=-2\frac{D\mu}{\mu}\ ,$$

$$H_{68}=-2\,\mathrm{Pr}(\gamma-1)M^2DW\ ,$$

$$H_{83}=\frac{R\,DW}{\mu T}-i\beta\left[l_1\frac{DT}{T}+\frac{D\mu}{\mu}\right],$$

$$H_{84}=i\frac{\beta R}{\mu}-\beta l_1\gamma M^2\xi\ ,\quad H_{85}=\beta l_1\frac{\xi}{T}-\frac{D(\mu' DW)}{\mu}\ ,$$

$$H_{86}=-DW\frac{\mu'}{\mu}\ ,\quad H_{87}=\alpha^2+\beta^2+i\frac{\xi R}{\mu T}\ ,$$

$$H_{88}=-\frac{D\mu}{\mu}\ .$$

Here $\xi = \alpha U + \beta W - \omega$ , $\chi = \left[\frac{R}{\mu} + il_2\gamma M^2\xi\right]^{-1}$ ,

$D = d/dy$ , $\mu' = d\mu/dT$ , $l_j = j + \lambda/\mu$ , $j = 1,2$ , $\mu$ и $\lambda$ – first and second viscosities respectively.

REFERENCES:


[1] V.N. Zhigulev, A.M. Tumin, *Turbulence origin.* Novosibirsk: Science, 1987.

[2] H.L. Reed, W.S. Saric, Stability of three-dimensional boundary layers, *Ann. Rev. Fluid Mech.*, Vol.21, 1989, pp.235–284.

[3] W.S. Saric, H.L. Reed, E.B. White, Stability and transition of three-dimensional boundary layers, *Annu.Rev.Fluid Mech.*, Vol.35, 2003, pp.413-440.

[4] S.G. Lekoudis, Stability of three-dimensional compressible boundary layers over wings with suction, AIAA Paper No. 79-0265, 1979.

[5] L.M. Mack, Compressible boundary layer stability calculations for sweptback wings with suction, *AIAA J*., Vol.20, No.3, 1982, pp. 363–369.

[6] Yu.G. Ermolaev, A.D. Kosinov, V.Ya. Levchenko, N.V. Semionov, Instability of a three-dimensional supersonic boundary layer, *J. Appl. Mech. Tech. Phys*., Vol.36, No.6, 1995, pp.840–843.

[7] H.L. Reed, W.S. Saric, Control of transition in supersonic boundary layers using distributed roughness – experiments and computations, *West East High Speed Flow Field*, Barselona, Spain, 2002, pp.417-425.

[8] N.V. Semionov, A.D. Kosinov, V.Ya. Levche–nko, Experimental study of turbulence beginning and transition control in a supersonic boundary layer on swept wing, in: *Laminar–Turbulent Transition*, Proc. of the 6th IUTAM symp., Bangalore (India), Dec. 13–17, 2004; Springer, New York, 2006, pp.355–362.

[9] A.D. Kosinov, N.V. Semionov, Yu.G. Ermolaev, V.Ya.Levchenko, Experimental study of evolution of disturbances in a supersonic boundary layer on a swept-wing model under controlled conditions, *J. Appl. Mech. Techn Phys.*, Vol.41, No.1, 2000, pp.44-49.

[10] N.V. Semionov, A.D. Kosinov, V.Ya. Levchenko, Experimental study of disturbance development in a 3D supersonic boundary layer, *West East High Speed Flow Field*, Marseille (France), Apr. 22–26, 2002; CIMNE, Barselona (2003), pp. 426–433.

[11] V.R. Gaponenko, A.V. Ivanov, Yu.S. Kacha–nov, Experimental investigation of swept wing boundary layer stability in relation to unsteady disturbances, *Thermophysics and Auromechanics*, Vol.2, No.4, 1995, pp.333-359.

[12] M. Asai, N. Saitoh, N. Itoh, Instability of compressible three-dimensional boundary layer to stationary disturbances. *Trans. Japan Soc. Aero. Space Sci.*, V.**43**, No.142,2001, pp.190-195.

[13] S.A. Gaponov, A.A. Maslov, *Development of disturbances in compressible flows*. Novosibirsk: Science, 1980.

[14] S.A. Gaponov, Interaction of External Vortical and Thermal Disturbances with Boundary Layer. *International Journal of Mechanics.* 2008, V.1. No.2, pp.15-19.

[15] M. Rahimpour, S.R. Mohebpour, A. Kimiaeifar, G.H.Bagheri, On the Analytical Solution of Axisymmetric Stagnation Flow Towards a Shrinking Sheet. *International Journal of Mechanics*, 2008, V.2, No.1, pp.1-10.

[16] D.H. Mccoy, X. Jiang, D. Lockerby, Analysis of Zero-Net-Mass-Flux Synthetic Jets using DNS. *WSEAS Transactions on Fluid Mechanics*, 2008, V.3, No.1, pp.47-55.

[17] A.M. Tumin, Nonlinear interaction in a three-7dimensional compressible boundary layer. *ICAS*-94, Anaheim, CA, 18-23 Sept 1994.

[18] S.A. Gaponov, B.V. Smorodsky, On the linear stability of supersonic boundary layer on a swept wing, 3rd Intern Summer Scientific Workshop "*High speed hydrodynamics and numerical simulation*", June 22-28, 2006, Kemerovo, Russia, pp.253-261.

[19] J.D. Anderson, *Modern Compressible Flow*, McGraw-Hill, New York, 1990.

[20] A.D. Kosinov, Yu.G. Ermolaev, N.V. Semio–nov, 'Anomalous' nonlinear wave phenomena in a supersonic boundary layer, *J. Appl. Mech. Tech. Phys.*, 1999, Vol.40, No.5, pp.858–864.

[21] S.A. Gaponov, N.M. Terekhova, Evolution of disturbances of elevated intensity in a supersonic boundary layer, *Aeromekh. Gaz. Dinamika*, 2003, No.1, pp.28–36.

[22] K. Kaups, T. Cebeci, Compressible laminar boundary layers with suction on swept and tapered wings. *J.Aircraft*, Vol.14, No.7, 1977, pp.661-667.